

A new approach to the numerical integration of rotational motion for interacting rigid bodies

Igor P. Omelyan

*Institute for Condensed Matter Physics, National Ukrainian Academy of Sciences,
1 Svientsitsky st., UA-290011 Lviv, Ukraine. E-mail: nep@icmp.lviv.ua*

Abstract

A new approach is developed to integrate numerically the equations of motion for systems of interacting rigid polyatomic molecules. With the aid of a leapfrog framework, we directly involve principal angular velocities into the integration, whereas orientational positions are expressed in terms of either principal axes or quaternions. As a result, the rigidness of molecules appears to be an integral of motion, despite the atom trajectories are evaluated approximately. In the case of microcanonical-ensemble dynamics, the approach leads to an algorithm which is free of any iterative procedures. It is shown that the algorithm derived exhibits significantly better properties in energy conservation with respect to all known rigid-body integrators. A thermostatted version is also described. It allows to obtain reliable results in computer simulations of water with huge time steps up to 10 fs, much larger than is usually possible.

MSC numbers: 65C20; 65-04; 68U20; 70E15; 82A71

Keywords: Numerical methods; Motion of rigid bodies; Long-time integration; Molecular dynamics simulation; Polyatomic molecules; Machine computation

I. INTRODUCTION

A lot of theories in physical chemistry treats the molecular liquid as a system of classical rigid bodies. The method of molecular dynamics (MD) remains the main tool for investigation of such a model. An important problem in MD simulations is the development of stable and efficient algorithms for integrating the equations of motion with orientational degrees of freedom. The straightforward parameterization of these degrees, Euler angles, is very inefficient for numerical calculations because of singularities inherent in the description [1–3]. Within singularity free approaches, the orientations of molecules typically are expressed in terms of quaternions [4–6]. High-order predictor-corrector Gear methods were utilized to integrate the rigid-body equations of motion in early investigations [7–10]. These multistep schemes are not reversible, and it is not clear that the extra order obtained is relevant, since they rather quickly become exhibit poor long-term stability of energy with increasing the step size [11].

Various alternatives to the Gear approach have been proposed and implemented over the years. These include the family of integrators comprising Verlet [12], velocity Verlet [13], leapfrog [14], and Beeman [15] methods, which are based on the Störmer central difference approximation [7, 16] of accelerations. Such integrators proved to be the most efficient, because high accuracy can be reached with minimal cost measured in terms of force evaluations. The main problem with these methods is that they were originally constructed, in fact, to integrate translational motion, assuming that accelerations are velocity-independent, and, therefore, additional modifications are necessary to use them for rotational dynamics. Analogous problems arise for charged particles moving in an external magnetic field.

In the atomic approach, the parameterization of orientational degrees of freedom can be circumvented by involving fundamental variables, namely, the individual Cartesian coordinates of atomic sites [11, 17–19]. As a result, the Störmer formula and its velocity leapfrog variant appear to be directly applicable. The dynamics is determined by integrating the equations of motion for these sites, subject to constraints that the intramolecular bond distances are fixed. Until now, the great majority of MD simulations

on rigid polyatomics are performed using the atomic-constraint technique due to its exceptional long-time stability. However, the application of this approach is inconvenient, in general, for several reasons. First, when there are more than two, three or four sites in the cases of linear, planar and three-dimensional molecules, respectively, the orientations cannot be defined uniquely. Second, as the number of atoms in each molecule is raised the number of constraints increases dramatically, decreasing the efficiency of the computations. Moreover, to exactly reproduce the rigid molecular structure, very complicated systems of nonlinear equations are needed to be solved at each time step of the integration process. An additional computational complexity arises in the force evaluations for intermolecular potentials that are not easily decomposable into direct site-site interactions such as potentials expressed through multi-pole expansions.

In order to obviate these difficulties, Ahlrichs and Brode have devised a hybrid method [20] in which the principal axes of molecules are considered as pseudo particles and constraint forces are introduced to maintain their orthonormality and, as a consequence, the molecular rigidity. The principal axes were evaluated within the Verlet framework via a recursive procedure which does not solve exactly the constraint equations to convergence, but instead writes the rotational matrix as an exponential for sum of some anti-symmetric matrices, restricting by a finite number of terms. A similar procedure has been used to adopt the pseudo-particle approach to velocity-Verlet and Beeman integrations [21]. It was established, however, that the exponential propagation leads to worse results on energy conservation than those obtained in the atomic-constraint technique. Such a situation can be explained by the fact that, although the omitted higher-order terms are in the self-consistency with the order of truncation errors for the algorithms used, they involve an unpredictable additional discrepancy in the evaluation of coordinates and the influence of this discrepancy appears to be significant already at relatively small values of the step size. Recently, acting in the spirit of the pseudo-particle formalism, a leapfrog-like algorithm has also been proposed [22]. In this algorithm the entire rotation matrix as well as the corresponding conjugate momentum are treated as dynamical variables, and the matrix of constraint forces is evaluated exactly. In such a way, the lost precision seems was reproduced, but this required again to find solutions by iteration to the systems of highly nonlinear

equations. The pseudo-particle and atomic approaches have yet a major disadvantage in that it is very hard to extend them to thermostatted versions. This is so, because the two problems on the conservation of temperature and molecular rigidity are coupled between themselves in a very complicated manner that prevents to resolve them in practice.

The first efforts on adopting the Störmer group of integrators to rotational motion in its pure form were done by Fincham [23–24]. As a result, rotational versions of the leapfrog algorithm have been proposed on the basis of equations of motion for angular momenta of molecules in the laboratory frame. In the case of a more accurate implicit version, the system of four nonlinear equations per molecule is solved by iteration for the same number of quaternion components [24]. To ensure the rigidness of molecules, the unit norm of quaternions was preserved using a rescaling method [9, 24]. As was soon realized [21, 25], angular-momentum versions are not very efficient at least in energy-conserving simulations, given that the artificial procedure is used to maintain the unit norm of quaternions and additional transformations with approximately computed rotational matrices and angular momenta are necessary to evaluate the principal components of angular velocities. Nevertheless, the chief achievement of rotational leapfrog versions was that they have allowed to perform thermostatted simulations on rigid polyatomics for the first time. The question of how to replace the crude quaternion renormalization by a more natural procedure has been considered too [25]. As a consequence, the quaternion dynamics with constraints was formulated and a new algorithm within the velocity Verlet framework was introduced. It has been shown [25, 26] that this algorithm conserves the total energy better than the implicit leapfrog integrator but not sufficiently.

Quite recently, to improve the stability, a new angular-velocity leapfrog algorithm for rigid-body simulations has been proposed [26]. Its main advantages were the intrinsic conservation of rigid structures and excellent stability properties. But a common drawback, existing in long-term stable integrators of rigid polyatomics, still remained, namely, the necessity to solve by iteration the systems of nonlinear equations. Although such equations are much simpler than those arising in the atomic and pseudo-particle approaches, the iterative solution should be considered as a negative feature.

In the present paper we develop the angular-velocity algorithm by avoiding any iterative procedures and show that the total energy can be conserved even better than within the cumbersome atomic technique. A thermostatted version of the algorithm is derived as well. We demonstrate that it gives the possibility to carry out simulations with extra large time steps, which are unaccessible in usual approaches.

II. THE ADVANCED LEAPFROG ALGORITHM

We shall deal with a classical collection of N identical rigid molecules composed of M point interaction sites. According to the molecular approach, the dynamics for such a system can be considered in view of translational and rotational motions. The translational motions is expressed in terms of the center of mass $\mathbf{r}_i = \sum_{a=1}^M m_a \mathbf{r}_i^a / m$ of each molecule $i = 1, \dots, N$, where \mathbf{r}_i^a denotes the positions of atomic site a within molecule i and $m = \sum_{a=1}^M m_a$ and m_a are the masses of a separate molecule and partial atoms, respectively. Then the translational part of the system evolution over time t can be determined in phase space by the $6N$ first-order differential equations

$$\frac{d\mathbf{r}_i}{dt} = \mathbf{v}_i, \quad m \frac{d\mathbf{v}_i}{dt} = \mathbf{f}_i \quad (1)$$

which represent the well-known Newton's law, where $\mathbf{f}_i = \sum_{j;a,b}^{N;M} \mathbf{f}_{ij}^{ab} (|\mathbf{r}_i^a - \mathbf{r}_j^b|)$ is the force acting on molecule i due to the site-site interactions \mathbf{f}_{ij}^{ab} with the other ($j \neq i$) molecules and \mathbf{v}_i designates the center-of-mass velocity.

A. Rotational motion in body-vector and quaternion representations

In the body-vector representation [4, 20, 21], the Cartesian coordinates of three principal axes XYZ of the molecule are assumed to be orientational variables. These variables can be collected into the 3×3 orthonormal matrices \mathbf{A}_i , so that the site positions in the laboratory frame are $\mathbf{r}_i^a(t) = \mathbf{r}_i(t) + \mathbf{A}_i^+(t) \Delta_a$, where $\Delta_a = (\Delta_X^a, \Delta_Y^a, \Delta_Z^a)^+$ is a vector-column of these positions in the body frame attached to the molecule and \mathbf{A}^+ denotes the matrix transposed to \mathbf{A} . The time-independent quantities Δ_a ($a = 1, \dots, M$) are completely defined by the rigid molecular structure. The rate of change in time of orientational matrices can be given as

$$\frac{d\mathbf{A}_i}{dt} = \begin{pmatrix} 0 & \Omega_Z^i & -\Omega_Y^i \\ -\Omega_Z^i & 0 & \Omega_X^i \\ \Omega_Y^i & -\Omega_X^i & 0 \end{pmatrix} \mathbf{A}_i \equiv \mathbf{W}(\boldsymbol{\Omega}_i) \mathbf{A}_i, \quad (2)$$

where Ω_X^i , Ω_Y^i and Ω_Z^i are principal components of the angular velocity $\boldsymbol{\Omega}_i$ and \mathbf{W} is a skewsymmetric matrix associated with $\boldsymbol{\Omega}_i$, i.e., $\mathbf{W}^+(\boldsymbol{\Omega}_i) = -\mathbf{W}(\boldsymbol{\Omega}_i)$.

In an alternative approach [4, 9], the matrix \mathbf{A}_i is a function,

$$\mathbf{A}(\mathbf{q}_i) = \begin{pmatrix} -\xi_i^2 + \eta_i^2 - \zeta_i^2 + \chi_i^2 & 2(\zeta_i\chi_i - \xi_i\eta_i) & 2(\eta_i\zeta_i + \xi_i\chi_i) \\ -2(\xi_i\eta_i + \zeta_i\chi_i) & \xi_i^2 - \eta_i^2 - \zeta_i^2 + \chi_i^2 & 2(\eta_i\chi_i - \xi_i\zeta_i) \\ 2(\eta_i\zeta_i - \xi_i\chi_i) & -2(\xi_i\zeta_i + \eta_i\chi_i) & -\xi_i^2 - \eta_i^2 + \zeta_i^2 + \chi_i^2 \end{pmatrix}, \quad (3)$$

of the four-component quaternion $\mathbf{q}_i \equiv (\xi_i, \eta_i, \zeta_i, \chi_i)^+$. The time derivatives of \mathbf{q}_i can be presented [26] in the form

$$\frac{d\mathbf{q}_i}{dt} = \frac{1}{2} \begin{pmatrix} 0 & \Omega_Z^i & -\Omega_X^i & -\Omega_Y^i \\ -\Omega_Z^i & 0 & -\Omega_Y^i & \Omega_X^i \\ \Omega_X^i & \Omega_Y^i & 0 & \Omega_Z^i \\ \Omega_Y^i & -\Omega_X^i & -\Omega_Z^i & 0 \end{pmatrix} \begin{pmatrix} \xi_i \\ \eta_i \\ \zeta_i \\ \chi_i \end{pmatrix} \equiv \frac{1}{2} \mathbf{Q}(\boldsymbol{\Omega}_i) \mathbf{q}_i, \quad (4)$$

where $\mathbf{Q}(\boldsymbol{\Omega}_i)$ is a skewsymmetric matrix again. The normalization condition $\mathbf{q}_i^2 = \xi_i^2 + \eta_i^2 + \zeta_i^2 + \chi_i^2 = 1$, which ensures the orthonormality $\mathbf{A}_i \mathbf{A}_i^+ = \mathbf{I}$ of $\mathbf{A}_i \equiv \mathbf{A}(\mathbf{q}_i)$, where \mathbf{I} designates the unit matrix, has been used to obtain Eq. (4). A consequence from the last conditions is that only three independent parameters are necessary to describe the nine elements of the orientational matrix and the four components of the quaternion.

The relations (2) and (4) for orientational coordinates need to be supplemented by the Euler's equations for angular velocities

$$\begin{aligned} J_X \frac{d\Omega_X^i}{dt} &= K_X^i + (J_Y - J_Z) \Omega_Y^i \Omega_Z^i, \\ J_Y \frac{d\Omega_Y^i}{dt} &= K_Y^i + (J_Z - J_X) \Omega_Z^i \Omega_X^i, \\ J_Z \frac{d\Omega_Z^i}{dt} &= K_Z^i + (J_X - J_Y) \Omega_X^i \Omega_Y^i, \end{aligned} \quad (5)$$

where J_α denote the time-independent moments inertia of the molecule along its principal axes ($\alpha = X, Y, Z$) and K_α^i are body-frame components, $\mathbf{K}_i = \mathbf{A}_i \mathbf{k}_i$, of the torque $\mathbf{k}_i = \sum_{j;a,b}^{N;M} (\mathbf{r}_i^a - \mathbf{r}_i) \times \mathbf{f}_{ij}^{ab}$ exerted on molecule i with respect to its center of mass.

In such a way, we obtain a coupled set of $6N$ translational (Eq. (1)) and $(9+3)N = 12N$ (Eqs. (2) and (5)) or $(4+3)N = 7N$ (Eqs. (4) and (5)) rotational first-order differential equations of motion, subject to $6N$ ($\{\mathbf{A}_i \mathbf{A}_i^+ = \mathbf{I}\}$) or N ($\{\mathbf{q}_i^2 = 1\}$) scalar constraints. If the equations of motion are solved exactly, these constraints will be conserved in time automatically.

B. Evaluation of angular velocities and coordinates

Let $\{\mathbf{r}_i(t), \mathbf{v}_i(t - \frac{h}{2}), \mathbf{S}_i(t), \boldsymbol{\Omega}_i(t - \frac{h}{2})\}$ be an initial spatially-velocity configuration of the system, where the velocities and positions are defined on alternate half-time steps with h being the fixed step size and $\mathbf{S}_i(t) \equiv \mathbf{A}_i(t)$ or $\mathbf{q}_i(t)$ are the orientational coordinates for the principal-axes or quaternion representations, respectively. The translational variables can be integrated applying the usual [14] leapfrog algorithm

$$\begin{aligned} \mathbf{v}_i(t + \frac{h}{2}) &= \mathbf{v}_i(t - \frac{h}{2}) + h \mathbf{f}_i(t)/m + \mathcal{O}(h^3), \\ \mathbf{r}_i(t + h) &= \mathbf{r}_i(t) + h \mathbf{v}_i(t + \frac{h}{2}) + \mathcal{O}(h^3) \end{aligned} \quad (6)$$

in which the molecular forces $\mathbf{f}_i(t)$ are explicitly evaluated in terms of known spatial coordinates $\mathbf{r}_i(t)$ and $\mathbf{S}_i(t)$. As can be verified easily, expanding the left- and right-hand sides of both the lines of Eq. (6) into Taylor series over h , the algorithm produces truncation single-step errors of order h^3 in coordinates and velocities (a more detailed discussion on local and global errors is presented in Appendix A).

In the case of rotational motion it is not a simple matter to adopt the standard leapfrog scheme, since the principal angular accelerations are velocity-dependent and the time derivatives of orientational coordinates depend not only on the angular velocity but also on the coordinates themselves. These problems were handled previously by Fincham [24] in his angular-momentum versions of the leapfrog algorithm. Recently [25, 26], it was shown that more superior techniques follow when the principal angular velocities, instead of angular momenta, are involved directly into the integration. Within the leapfrog framework, mid-step values for the angular velocities can be evaluated by writing

$$\Omega_\alpha^i(t + \frac{h}{2}) = \Omega_\alpha^i(t - \frac{h}{2}) + h \left[K_\alpha^i(t) + (J_\beta - J_\gamma) \Omega_\beta^i(t) \Omega_\gamma^i(t) \right] / J_\alpha + \mathcal{O}(h^3), \quad (7)$$

where Euler equations (5) have been taken into account, (α, β, γ) denote an array of three cyclic permutations for (X, Y, Z) and the molecular torques $K_\alpha^i(t)$ are computed via the coordinates $\mathbf{r}_i(t)$ and $\mathbf{S}_i(t)$. Equation (7) presents a rotational-motion analog for the first line of (6) but it must be complemented by a propagation of the products of angular velocities to on-step levels of time. It is quite naturally to perform such a propagation in the form

$$\Omega_\beta^i(t)\Omega_\gamma^i(t) = \frac{1}{2} \left[\Omega_\beta^i(t - \frac{h}{2})\Omega_\gamma^i(t - \frac{h}{2}) + \Omega_\beta^i(t + \frac{h}{2})\Omega_\gamma^i(t + \frac{h}{2}) \right] + \mathcal{O}(h^2), \quad (8)$$

where the second-order accuracy is in the self-consistency with the third-order truncation errors arising when evaluating angular velocities. In view of the last equality, vector expression (7) is an implicit equation with respect to $\Omega_i(t + \frac{h}{2})$, which allows to be solved by iteration [26]. But an essential advantage of the approach presented lies in the fact that the solutions to (7) can be cast in quadratures without applying any iterative procedures. This question will be considered in the next subsection.

Analogously to the second line of the translational-motion algorithm (6), we evaluate orientational coordinates,

$$\mathbf{S}_i(t + h) = \mathbf{S}_i(t) + h \mathbf{H}_i(t + \frac{h}{2}) \mathbf{S}_i(t + \frac{h}{2}) + \mathcal{O}(h^3), \quad (9)$$

for the cases of principal-axis vectors ($\mathbf{S}_i \equiv \mathbf{A}_i, \mathbf{H}_i \equiv \mathbf{W}_i$) and quaternion ($\mathbf{S}_i \equiv \mathbf{q}_i, \mathbf{H}_i \equiv \frac{1}{2}\mathbf{Q}_i$) representations, where Eqs. (2) and (4) have been used. The matrices $\mathbf{W}_i \equiv \mathbf{W}(\Omega_i)$ and $\mathbf{Q}_i \equiv \mathbf{Q}(\Omega_i)$ are only velocity-dependent and they are calculated in (9) using the already defined values of $\Omega_i(t + \frac{h}{2})$, whereas the obvious choice for mid-step values of the orientational variables is

$$\mathbf{S}_i(t + \frac{h}{2}) = \frac{1}{2} [\mathbf{S}_i(t) + \mathbf{S}_i(t + h)] + \mathcal{O}(h^2). \quad (10)$$

Equations (9) and (10) constitute, in fact, a system of linear equations with respect to elements of $\mathbf{A}_i(t + h)$ or $\mathbf{q}_i(t + h)$, which, is solved analytically,

$$\mathbf{S}_i(t + h) = [\mathbf{I} - \frac{h}{2}\mathbf{H}_i(t + \frac{h}{2})]^{-1} [\mathbf{I} + \frac{h}{2}\mathbf{H}_i(t + \frac{h}{2})] \mathbf{S}_i(t) + \mathcal{O}(h^3), \quad (11)$$

where it is understood that \mathbf{I} designates either three- or four-dimensional unit matrix in the principal axes or quaternion domains, respectively.

The single integration process described can be repeated for the next time step, shifting the initial time t to $t + h$. In such a way, step by step ($n = 1, 2, \dots$) the dynamics $\{\mathbf{r}_i(t + nh), \mathbf{v}_i(t + (n - \frac{1}{2})h), \mathbf{S}_i(t + nh), \boldsymbol{\Omega}_i(t + (n - \frac{1}{2})h)\}$ of the system is numerically evaluated.

Taking into account expressions (2) and (4) for matrix \mathbf{H}_i , the result (11) can be written more explicitly,

$$\begin{aligned}\mathbf{A}_i(t + h) &= \frac{\mathbf{I}[1 - \frac{h^2}{4}\Omega_i^2(t + \frac{h}{2})] + h\mathbf{W}_i + \frac{h^2}{2}\mathbf{P}_i}{1 + \frac{h^2}{4}\Omega_i^2(t + \frac{h}{2})} \mathbf{A}_i(t) \equiv \mathbf{D}_i(t, h) \mathbf{A}_i(t), \\ \mathbf{q}_i(t + h) &= \frac{\mathbf{I}[1 - \frac{h^2}{16}\Omega_i^2(t + \frac{h}{2})] + \frac{h}{2}\mathbf{Q}_i}{1 + \frac{h^2}{16}\Omega_i^2(t + \frac{h}{2})} \mathbf{q}_i(t) \equiv \mathbf{G}_i(t, h) \mathbf{q}_i(t),\end{aligned}\quad (12)$$

where $[\mathbf{P}_i]_{\alpha\beta} = \Omega_\alpha^i \Omega_\beta^i$ denotes a symmetric matrix which, as the matrices \mathbf{W}_i and \mathbf{Q}_i , is computed in (12) using the angular velocities at the middle-step time $t + \frac{h}{2}$. It can be checked that the matrix $(\mathbf{I} - \epsilon\mathbf{H})^{-1}(\mathbf{I} + \epsilon\mathbf{H})$ is orthonormal at arbitrary values of ϵ , provided $\mathbf{H}^+ = -\mathbf{H}$. Therefore, the 3×3 and 4×4 evolution matrices \mathbf{D}_i and \mathbf{G}_i are orthonormal by construction as well. Using the equalities $\mathbf{W}_i^2 = \mathbf{P}_i - \Omega_i^2\mathbf{I}$ and $\mathbf{Q}_i^2 = -\Omega_i^2\mathbf{I}$, these matrices can be presented in the exclusive compact forms

$$\begin{aligned}\mathbf{D}_i(t, h) &= \exp[\varphi_i \mathbf{W}_i / \Omega_i]_{t+\frac{h}{2}}, \quad \varphi_i = \arcsin \frac{h\Omega_i(t + \frac{h}{2})}{1 + \frac{h^2}{4}\Omega_i^2(t + \frac{h}{2})}, \\ \mathbf{G}_i(t, h) &= \exp[\phi_i \mathbf{Q}_i / \Omega_i]_{t+\frac{h}{2}}, \quad \phi_i = \arcsin \frac{h\Omega_i(t + \frac{h}{2})}{2 + \frac{h^2}{8}\Omega_i^2(t + \frac{h}{2})},\end{aligned}\quad (13)$$

where **exp** designates the matrix exponential. From Eq. (13) it becomes clear that the matrices \mathbf{D}_i and \mathbf{G}_i define three- and four-dimensional rotations on angles φ_i and ϕ_i in the laboratory frame and quaternion space, respectively. In the first case the rotation is performed around the unit vector $\boldsymbol{\Omega}_i / \Omega_i|_{t+\frac{h}{2}}$, whereas in the second one it is carried out around a virtual orth which is perpendicular to all four orths of the quaternion space.

As far as the evolution matrices are rotational ones, the following statement emerges immediately. If initially the orthonormality of \mathbf{A}_i and the unit norm of \mathbf{q}_i are fulfilled, they will be satisfied perfectly in future, despite an approximate character of the evaluated coordinate trajectories $\{\mathbf{r}_i(t + nh), \mathbf{S}_i(t + nh)\}$. This excellent property distin-

guishes the algorithm introduced from all other singularity-free algorithms known, since no artificial or constraint normalizations as well as no recursive or iterative procedures are necessary to conserve the rigidness of molecules.

It is worth remarking that the quaternion and body-vector treatments are completely identical with respect to produced atom trajectories if the corresponding equations of rotational motion are solved precisely. In our leapfrog scheme the trajectories will differ between themselves by terms of orders h^3 and higher, i.e., $\mathbf{A}_i[\mathbf{q}_i(t+h)] - \mathbf{A}_i(t+h) = \mathcal{O}(h^3)$ (if initially $\mathbf{A}_i[\mathbf{q}_i(t)] = \mathbf{A}_i(t)$) or, in other words, $\mathcal{D}_i(t, h) - \mathbf{D}_i(t, h) = \mathcal{O}(h^3)$, where $\mathcal{D}_i(t, h) = \mathbf{A}_i[\mathbf{q}_i(t+h)]\mathbf{A}_i^+(t)$. That is very interesting, the matrix $\mathcal{D}_i(t, h)$ describes the rotation around the same vector as the propagator $\mathbf{D}_i(t, h)$, but on a somewhat different angle $\varphi'_i = \varphi_i + \mathcal{O}(h^3)$. We see, therefore, that the uncertainties are the same order as truncation terms of the algorithm. From this point of view, both the representations can be applied to numerical computations with equal success. However, the implicit computation $\mathbf{A}_i[\mathbf{q}_i(t+h)]$ (via Eq. (3)) of orientational matrices in terms of quaternions (the second line of Eq. (12)) requires less elementary arithmetical operations to be executed and also less memory to be saved ($4N$ units, instead of $9N$ ones) for orientational positions than in the case of direct computation (the first line of (12)) that may be important in some applications of the algorithm.

C. Quasianalytical solutions for angular velocities

We shall show in this subsection how to perform analytically the evaluation of principal angular velocities in our advanced leapfrog algorithm. The system (Eqs. (7) and (8)) of three equations per molecule is needed to be solved with respect to the same number of unknowns $\Omega_\alpha^i(t + \frac{h}{2})$, where $\alpha = X, Y, Z$, during such an evaluation. First of all it is necessary to point out that the equations are nonlinear only when all the principal moments of inertia are different, i.e., when $J_X \neq J_Y \neq J_Z$. Let us consider now this more difficult case (specific examples are described in Subsect. II D). We notice that the first two equations ($\alpha = X, Y$) of system (7) appear to be linear with respect to $\Omega_X^i(t + \frac{h}{2})$ and $\Omega_Y^i(t + \frac{h}{2})$ which, therefore, can easily be expressed in terms of $\Omega_Z^i(t + \frac{h}{2})$. The result is

$$\Omega_X^i(t + \frac{h}{2}) = \frac{\theta_X + h\rho_X\theta_Y\Omega_Z^i(t + \frac{h}{2})}{1 + h^2\mu^2\Omega_Z^{i,2}(t + \frac{h}{2})}, \quad \Omega_Y^i(t + \frac{h}{2}) = \frac{\theta_Y + h\rho_Y\theta_X\Omega_Z^i(t + \frac{h}{2})}{1 + h^2\mu^2\Omega_Z^{i,2}(t + \frac{h}{2})}, \quad (14)$$

where $\theta_\alpha = \Omega_\alpha^i(t - \frac{h}{2}) + [K_\alpha^i(t)/J_\alpha + \rho_\alpha\Omega_\beta^i(t - \frac{h}{2})\Omega_\gamma^i(t - \frac{h}{2})]h$, $\rho_\alpha = (J_\beta - J_\gamma)/(2J_\alpha)$ and $0 < \mu^2 = -\rho_X\rho_Y \leq 1/4$. The last inequalities follow from the requirements $J_\alpha > 0$ and $J_\alpha \leq J_\beta + J_\gamma$ imposed on principal moments of inertia.

Substituting the result (14) for $\Omega_X^i(t + \frac{h}{2})$ and $\Omega_Y^i(t + \frac{h}{2})$ into the third equation ($\alpha = Z$) of system (7) and presenting the Z -th component of the angular velocity as $\Omega_Z^i(t + \frac{h}{2}) = s_0 + \delta$ yields the following algebraic equation

$$a_0 + a_1\delta + a_2\delta^2 + a_3\delta^3 + a_4\delta^4 + a_5\delta^5 = 0 \quad (15)$$

with the coefficients

$$\begin{aligned} a_0 &= (s_0 - \theta_Z)\vartheta_+^2 - h\rho_Z[\theta_X\theta_Y\vartheta_- + h(\rho_Y\theta_X^2 + \rho_X\theta_Y^2)s_0], \\ a_1 &= \vartheta_+ - h^2\{(\rho_Y\theta_X^2 + \rho_X\theta_Y^2)\rho_Z - \mu^2s_0[(5s_0 - 4\theta_Z)\vartheta_+ + 2h\theta_X\theta_Y\rho_Z]\}, \\ a_2 &= h^2\mu^2[6s_0 - 2\theta_Z + h\rho_Z\theta_X\theta_Y + h^2\mu^2s_0^2(10s_0 - 6\theta_Z)], \\ a_3 &= 2h^2\mu^2[1 + h^2\mu^2s_0(5s_0 - 2\theta_Z)], \\ a_4 &= h^4\mu^4(5s_0 - \theta_Z), \quad a_5 = h^4\mu^4, \end{aligned} \quad (16)$$

where $\vartheta_\pm = 1 \pm h^2\mu^2s_0^2$. The equation (15) is fifth order and the corresponding solutions for $\Omega_Z^i(t + \frac{h}{2})$ are independent on the parameter s_0 , provided the unknown δ is precisely determined. However, as is well known, only algebraic equations of fourth or less orders allow to be solved in quadratures completely.

The main idea of quasianalytical solutions consists in the fact that actual MD simulations are performed with relative small values of the time step h . Then it is necessary to choose the parameter s_0 as a good prediction for $\Omega_Z^i(t + \frac{h}{2})$ to be entitled to ignore high-order terms in the left-hand side of Eq. (15). The simplest choice for this can be found assuming that the nonlinear velocity term in the right-hand side of Eq. (7) at $\alpha = Z$ is time-independent during the interval $[t - \frac{h}{2}, t]$, i.e., putting $\Omega_X^i(t)\Omega_Y^i(t) = \Omega_X^i(t - \frac{h}{2})\Omega_Y^i(t - \frac{h}{2}) + \mathcal{O}(h)$. As a result, one obtains

$$s_0 = \theta_Z + \rho_Z\Omega_X^i(t - \frac{h}{2})\Omega_Y^i(t - \frac{h}{2})h \quad (17)$$

that represents the original values of $\Omega_Z^i(t + \frac{h}{2})$ with the second-order truncation error, so that $\delta = \mathcal{O}(h^2)$. It is easy to see that in this case the two last terms $a_4\delta^4$ and

$a_5\delta^5$ in the left-hand side of Eq. (15) behaves as $\mathcal{O}(h^{12})$ and $\mathcal{O}(h^{14})$, respectively. Taking into account the smallness of h , such terms can merely be omitted without any loss of the precision, because they involve uncertainties of order $\mathcal{O}(h^{12})$ and higher into the desired solution and appear to be too small with respect to the third-order truncation errors $\mathcal{O}(h^3)$ involved previously in angular velocities by the algorithm. These omitted terms can even be minimized yet, provided $J_X \neq J_Y > J_Z$. Indeed, then the X - and Y -th components of the angular velocity are the most slow variables and estimation (17) for $\Omega_Z^i(t + \frac{h}{2})$ becomes more accurate, decreasing the deviation $|\delta|$. Moreover, at given values of J_X , J_Y and J_Z , the multiplier μ^2 riches a minimum when $\min_{\alpha=X,Y,Z} |J_\alpha| = J_Z$, decreasing the influence of the highest-order coefficients again. That is why the algebraic equation must be constructed with respect to the component Ω_Z^i associated with the least value for principal moments of inertia.

Eq. (15) is now transformed to the third-order algebraic equation

$$a_0 + a_1\delta + a_2\delta^2 + a_3\delta^3 = \mathcal{O}(h^{12}) \quad (18)$$

which can easily be solved analytically. The result is

$$\begin{aligned} \delta_1 &= -\frac{1}{3}a_2/a_3 + c - b/c + \mathcal{O}(h^{12}), \\ \delta_{2,3} &= -\frac{1}{3}a_2/a_3 - \frac{1}{2}[c - b/c \pm i\sqrt{3}(c + b/c)] + \mathcal{O}(h^{12}), \end{aligned} \quad (19)$$

where

$$\begin{aligned} b &= \frac{1}{9}(3a_1a_3 - a_2^2)/a_3^2, \\ c &= (p + \sqrt{b^3 + p^2})^{1/3}, \\ p &= \frac{1}{54}(9a_1a_2a_3 - 27a_0a_3^2 - 2a_2^3)/a_3^3. \end{aligned} \quad (20)$$

Among the three solutions only the first one δ_1 is real and satisfies the physical boundary condition $\sim h^2$ when h goes to zero (the other two solutions $\delta_{2,3}$ are purely imaginary at $h \rightarrow 0$ and they tend to infinity as $\sim \pm i/h$).

Therefore, the desired Z -th component of the angular velocity is

$$\Omega_Z^i(t + \frac{h}{2}) = s_0 + \delta_1. \quad (21)$$

The rest two components $\Omega_X^i(t + \frac{h}{2})$ and $\Omega_Y^i(t + \frac{h}{2})$ can be reproduced on the basis of equalities (14).

D. Integration in specific cases

Although the algorithm derived can be applied to arbitrary rigid polyatomics, some simplifications are possible using special properties of the molecule. The simplest case is molecules with a spherical distribution of mass, when all the moments of inertia are equal, i.e., $J_X = J_Y = J_Z \equiv J$ and arbitrary tree perpendicular between themselves axes can be chosen as principal ones at an initial time. Then, no velocity-dependent contributions into the torques (the second terms in the right-hand sides of equation (5)) appear and it is more convenient to work within the body-vector representation and to rewrite the equations of rotational motion (2) and (5) in terms of the angular velocity $\boldsymbol{\omega}_i = \mathbf{A}_i^+ \boldsymbol{\Omega}_i$ in the laboratory frame, i.e., $d\mathbf{A}_i/dt = \mathbf{W}^+(\boldsymbol{\omega}_i)\mathbf{A}_i$ and $Jd\boldsymbol{\omega}_i/dt = \mathbf{k}_i$. The leapfrog trajectories for these equations are obvious: $\boldsymbol{\omega}_i(t + \frac{h}{2}) = \boldsymbol{\omega}_i(t - \frac{h}{2}) + \frac{h}{J} \mathbf{k}_i(t)$ and $\mathbf{A}_i(t + h) = \exp[-\varphi_i \mathbf{W}_i(\boldsymbol{\omega}_i)/\omega_i]_{t+\frac{h}{2}} \mathbf{A}_i(t)$, where $\varphi_i = \arcsin[h\omega_i/(1 + \frac{h^2}{4}\omega_i^2)]_{t+\frac{h}{2}}$.

For some particular models, the orientational part of the intermolecular potential can be expressed using only unit three-component vectors $\boldsymbol{\rho}_i$ passing through the centers of mass of molecules. The examples are point dipole interactions, when $\boldsymbol{\rho}_i \equiv \boldsymbol{\nu}_i/\nu_i$ with $\boldsymbol{\nu}_i$ being the dipole moment, or when all force sites of the molecule are aligned along $\boldsymbol{\rho}_i$. If then additionally the condition $J_{X,Y,Z} = J$ is satisfied (for the last example this can be possible when forceless mass sites are placed in such a way to ensure the spherical mass distribution), it is no longer necessary to deal with orientational matrices or quaternions. In this case the equation for $\boldsymbol{\rho}_i$ looks as $d\boldsymbol{\rho}_i/dt = \mathbf{W}^+(\boldsymbol{\omega}_i)\boldsymbol{\rho}_i$ with the solution $\boldsymbol{\rho}_i(t + h) = \exp[-\varphi_i \mathbf{W}_i(\boldsymbol{\omega}_i)/\omega_i]_{t+\frac{h}{2}} \boldsymbol{\rho}_i(t)$.

For molecules with cylindric distribution of mass sites, when two of three of principal moments of inertia are equal, the numerical trajectory can also be determined in a simpler manner. Let us assume for definiteness that $J_X = J_Y \neq J_Z$ and $J_Z \neq 0$. Then arbitrary two perpendicular between themselves axes, lying in the plane perpendicular to Z -th principal axis, can be chosen initially as X - and Y -th principal orths. The corresponding solution to Eq. (7) at $\alpha = Z$ is found now exactly, namely, $\Omega_Z^i(t + \frac{h}{2}) = \Omega_Z^i(t - \frac{h}{2}) + \frac{h}{J_Z} K_Z^i(t)$ and, as in the general case, the values for components X and Y of the angular velocity are evaluated on the basis of Eq. (14), whereas the orientational matrices or quaternions are computed via Eq. (12).

A special attention should be paid on linear molecules when $J_X = J_Y = J \neq J_Z = 0$. Each such molecule has two, instead of free, orientational degrees of freedom and to reproduce a correct dynamics by Euler equations it is necessary to put formally $\Omega_Z^i \equiv 0$ to exclude nonexistent torques caused by irrelevant rotations of the molecule around Z -axis. Then, as it follows from Eq. (14), we have $\Omega_X^i(t + \frac{h}{2}) = \Omega_X^i(t - \frac{h}{2}) + \frac{h}{J} K_X^i(t)$ and $\Omega_Y^i(t + \frac{h}{2}) = \Omega_Y^i(t - \frac{h}{2}) + \frac{h}{J} K_Y^i(t)$. Planar molecules do not present a specific case within our approach and they should be handled in the usual way similarly to three-dimensional bodies. The integration in the presence of an external electromagnetic field is considered in Appendix B.

III. THERMOSTATTED VERSIONS

Since the velocities appear explicitly in our approach, it is possible to introduce various thermostats to simulate canonical ensembles. As is well known [24, 27], thermostatted versions allow to perform simulations with significantly greater step sizes than those used within the energy-conserving dynamics. In canonical ensembles the time evolution is determined provided the temperature $T = 2\Gamma/(lNk_B)$ of the system is an integral of motion, where Γ and k_B are the kinetic energy and the Boltzmann's constant, respectively. The number l of degrees of freedom per particle is equal to 6 for arbitrary rigid polyatomics, except the cases of linear molecules ($l = 5$) and pure translational motion ($l = 3$).

The simplest thermostatted version is based on the estimation of on-step translational velocities

$$\mathbf{v}_i(t) = \frac{1}{2} \left[\mathbf{v}_i(t - \frac{h}{2}) + \mathbf{v}_i(t + \frac{h}{2}) \right] + \mathcal{O}(h^2), \quad (22)$$

commonly used to calculate the kinetic part $\Gamma(\{\mathbf{v}_i(t)\}) \equiv \Gamma(t) = \frac{1}{2} \sum_{i=1}^N m \mathbf{v}_i^2(t)$ of the total energy and, as a consequence, the temperature $T(t)$ at time t during the standard leapfrog step (6). Then, velocities (22) are modified as $\mathbf{v}'_i(t) = \beta \mathbf{v}_i(t)$ using the scaling factor $\beta = \sqrt{T_0/T}$, where T_0 is the required constant temperature [28]. The velocity integration is completed by

$$\mathbf{v}'_i(t + \frac{h}{2}) = (2 - \beta^{-1}) \mathbf{v}'_i(t) + \frac{h}{2} \mathbf{f}_i(t)/m \quad (23)$$

which satisfies $\mathbf{v}'_i(t) = \frac{1}{2}[\mathbf{v}_i(t - \frac{h}{2}) + \mathbf{v}'_i(t + \frac{h}{2})]$ and $T(\{\mathbf{v}'_i(t)\}) = T_0$. Similar modifications are obtained within the angular-momentum algorithms [24].

In our case it is not so obvious to extend the angular-velocity algorithm to a thermostatted version on the basis of such rather intuitive grounds, because the angular accelerations are velocity-dependent. For this reason we consider first the question how to reproduce result (23) in the framework of a more consequent approach. The main idea lies in the following. In the thermostat the velocities are not independent and constrained by the condition $\Gamma = \text{const}$. The last equality can be satisfied introducing the generalized friction forces $-\lambda(t)\nabla_{\mathbf{v}_i}\Gamma = -\lambda(t)m\mathbf{v}_i(t)$. These virtual forces are now added to the real ones and, as a result, solution (6) for translational velocities transforms into

$$\mathbf{v}_i(t + \frac{h}{2}) = \mathbf{v}_i(t - \frac{h}{2}) + h[\mathbf{f}_i(t) - \lambda(t)m\mathbf{v}_i(t)]/m + \mathcal{O}(h^3), \quad (24)$$

where on-step velocities $\mathbf{v}_i(t)$ match Eq. (22). Solving equation (24) with respect to $\mathbf{v}_i(t)$ and satisfying the condition $T(t) \equiv T(\{\mathbf{v}_i(t)\}) = T_0$ leads to a single quadratic equation for the friction coefficient λ with the solutions $-2(1 \mp \beta^{-1})/h$. Because of $\lim_{h \rightarrow 0} \beta \rightarrow 1$, the second solution behaves like $4/h$ and should be rejected. Only the first solution $-2(1 - \beta^{-1})/h$ is acceptable from the physical point of view. It tends to the finite value $\lambda_0(t) = \sum_{i=1}^N \mathbf{v}_i(t) \cdot \mathbf{f}_i(t) / (lNk_B T_0)$ when h goes zero, indicating about the third-order truncation errors in (24) despite the second-order estimation (22) and automatically fulfilling the condition $d\Gamma/dt = \sum_{i=1}^N \mathbf{v}_i \cdot [\mathbf{f}_i - \lambda_0 m \mathbf{v}_i] = 0$, which follows from $\Gamma = \text{const}$. As can be verified by straightforward calculations, equation (24) is equivalent to (23) when $\lambda(t) = -2(1 - \beta^{-1})/h$.

In such a manner, the temperature of the system is conserved exactly at on-step levels of time during the leapfrog trajectories, i.e., $T(t + (n-1)h) = T_0$, whereas it will differ slightly from the requested value by terms of order h^3 and higher at mid step times, i.e., $T(t + (n-1/2)h) = T_0 + \mathcal{O}(h^3)$, being in the self-consistency with the same order of truncation errors for velocities (24).

Consider now the angular-velocity integration within the generalized friction formalism. For rigid molecules the kinetic energy consists of translational and rotational parts, $\Gamma = \frac{1}{2} \sum_{i=1}^N [m\mathbf{v}_i^2 + \sum_{\alpha}^{X,Y,Z} J_{\alpha} \Omega_{\alpha}^i]^2$. In this case the condition $\Gamma = \text{const}$ requires

the introduction of additional friction torques, $-\lambda(t)\partial\Gamma/\partial\Omega_\alpha^i = -\lambda(t)J_\alpha\Omega_\alpha^i(t)$, together with the translational friction forces described above. Then, using the estimation of on-step angular velocities

$$\boldsymbol{\Omega}_i(t) = \frac{1}{2}\left[\boldsymbol{\Omega}_i(t - \frac{h}{2}) + \boldsymbol{\Omega}_i(t + \frac{h}{2})\right] + \mathcal{O}(h^2), \quad (25)$$

needed to computer the friction torques, and collecting two terms of the real torque acting on molecule i into the one vector \mathbf{L}_i with the components

$$L_\alpha^i(t) = K_\alpha^i(t) + \frac{1}{2}(J_\beta - J_\gamma) \left[\Omega_\beta^i(t - \frac{h}{2})\Omega_\gamma^i(t - \frac{h}{2}) + \Omega_\beta^i(t + \frac{h}{2})\Omega_\gamma^i(t + \frac{h}{2}) \right], \quad (26)$$

we modify equation (7) as

$$\Omega_\alpha^i(t + \frac{h}{2}) = \{[1 - \lambda\frac{h}{2}]\Omega_\alpha^i(t - \frac{h}{2}) + hL_\alpha^i(t)/J_\alpha\}/[1 + \lambda\frac{h}{2}]. \quad (27)$$

The translational-velocity part of the thermostatted dynamics can be proceeded, rewriting Eq. (24) in the following equivalent form

$$\mathbf{v}_i(t + \frac{h}{2}) = \{[1 - \lambda\frac{h}{2}]\mathbf{v}_i(t - \frac{h}{2}) + h\mathbf{f}_i(t)/m\}/[1 + \lambda\frac{h}{2}]. \quad (28)$$

The generalized friction coefficient λ , arising in Eqs. (27) and (28), is found to provide the temperature constant. For example, we can apply the usual on-step constant-temperature scheme for which $T(t) = T_0$. In our algorithm, it appears to be more convenient to conserve the temperature at mid-step levels of time. The last scheme looks more naturally within the leapfrog framework, because the velocities are really generated at these levels and no additional interpolations like (22) and (25) are necessary to computer the temperature. In the energy-conserving dynamics, such interpolations are commonly used to synchronize kinetic and potential parts of the total energy to the same times. Thermostatted calculations are not needed in this synchronization given that the total energy fluctuations are completely determined by correlations of the potential energy. It is worth emphasizing also that the mid-step constant-temperature scheme cannot be applied directly to angular-momentum algorithms [24], where the angular velocities are not well defined quantities at middle time steps.

Thus, putting $T(t + \frac{h}{2}) = T_0$ and considering the nonlinear terms $\Omega_\beta^i(t + \frac{h}{2})\Omega_\gamma^i(t + \frac{h}{2})$ in the right-hand side of Eq. (26) as parameters, yields a linear equation with respect

to λ , provided $T(t - \frac{h}{2}) = T_0$. The last condition is not self-starting and this must be taken into account at the generation of angular velocities at the very beginning of the integration process. The solution of the linear equation is

$$\lambda \equiv \lambda(\{\boldsymbol{\Omega}_i(t + \frac{h}{2})\}) = 2 \frac{\Lambda_1 + h\Lambda_2}{T_0 + h\Lambda_1}, \quad (29)$$

where

$$\begin{aligned} \Lambda_1 &= \frac{1}{2lNk_B} \sum_{i=1}^N [\mathbf{v}_i(t - \frac{h}{2}) \cdot \mathbf{f}_i(t) + \boldsymbol{\Omega}_i(t - \frac{h}{2}) \cdot \mathbf{L}_i(t)], \\ \Lambda_2 &= \frac{1}{4lNk_B} \sum_{i=1}^N [\mathbf{f}_i^2(t)/m + \sum_{\alpha}^{X,Y,Z} L_{\alpha}^i(t)/J_{\alpha}]. \end{aligned} \quad (30)$$

The vector equation (27) in view of expressions (26) and (29) constitutes a system of three equations per molecule for the same number of unknowns $\Omega_{\alpha}^i(t + \frac{h}{2})$. The system of equations can now be solved iteratively, putting initially $\boldsymbol{\Omega}_i(t - \frac{h}{2})$, instead of $\boldsymbol{\Omega}_i(t + \frac{h}{2})$, in all nonlinear terms which are collected in the right-hand side of (27). The obtained values for $\boldsymbol{\Omega}_i(t + \frac{h}{2})$ in the left-hand side of (27) are considered as initial guess for the next iteration (note that no iterations are necessary for linear or spherically symmetric molecules, because then nonlinear terms are absent, and Eq. (27) presents an explicit equation for the angular velocity). The convergence of iterations is justified by the smallness of h which always is meet in actual MD simulations. It is necessary to point out that the multiplier λ (Eqs. (29) and (30)) depends nonlinearly on angular velocities of all molecules. Therefore, to take the next iteration we must complete the previous one for each molecule and then recalculate λ . When the required iterative precision is achieved, the iterations are stopped and the obtained angular velocities $\boldsymbol{\Omega}_i(t + \frac{h}{2})$ are used to calculate a final value for λ . Then this value is substituted into Eq. (28) to evaluate new translational velocities $\mathbf{v}_i(t + \frac{h}{2})$. The coordinates $\mathbf{S}_i(t + h)$ and $\mathbf{r}_i(t + h)$ are updated according to the same rules (see Eq. (12) and the second line of Eq. (6)) as for energy-conserving dynamics.

The existence of the generalized friction coefficient $\lambda(t)$ makes the time evolution of the system to be irreversible. This coefficient can accept positive as well as negative values. As in the case of real mechanical friction, the positive values will correspond to decreasing the total energy of the system. At negative values a portion of the energy is transferred from the thermostat to the system.

IV. MD TESTS. COMPARISON WITH PREVIOUS METHODS

The system chosen was the TIP4P model of water [29] at a density of $mN/V = 1 \text{ g/cm}^3$ and temperature of $T=298 \text{ K}$. Such a system should provide a very severe test for rotational algorithms because of the low moments of inertia of the molecule and the large torques due to the site-site interactions. To reduce cut-off effects we used a cubic sample of $N = 256$ molecules and the reaction field geometry [30]. When evaluating molecular forces and torques, intersite components of the TIP4P potential were cut off and shifted to zero at the truncation point to avoid the system energy drift associated with the passage of sites through the surface of the cut-off sphere. The cut-off radius was at half the box length. Our MD programs were implemented in Fortran language using double precision throughout. They were executed on a Pentium-S 120 MHz personal computer at around 0.8 s per time step. All runs were started from an identical well equilibrated configuration.

A. Energy-conserving dynamics

One of the most important tests to verify that MD simulations in microcanonical (NVE) ensembles are proceeding correctly is the test on conservation of the total energy of the system. Since the coordinates and velocities are evaluated approximately within a particular algorithm, the total energy will not conserve exactly. Instead, it will oscillate around a constant level or even deviate significantly when the numerical solutions are produced with insufficient accuracy. To reproduce features of an NVE ensemble properly, it is necessary for the ratio $\Upsilon = \mathcal{E}/\mathcal{U}$ of the total energy fluctuations $\mathcal{E} = [\langle (E - \langle E \rangle)^2 \rangle]^{1/2}/|\langle E \rangle|$ to the corresponding fluctuations \mathcal{U} of the potential energy, averaged along the generated phase trajectory, to be no more than a few per cent. The total energy $E = \Gamma + U$ consists of the kinetic Γ and potential U parts. Thus, the computation of E at time t within a leapfrog framework requires the knowledge of on-step velocities. These velocities can be calculated using estimators (22) and (25), where the main term $\mathcal{O}(h^2)$ of uncertainties is in law with the second order of global errors for our algorithm (see Appendix A).

We have made comparative tests performing MD runs on the basis of our advanced leapfrog algorithm within quaternion and principal-axes variables, as well as all other approaches of which we are aware. They are the fifth-order Gear integrator [7], implicit leapfrog algorithm of Fincham [24], pseudo-site formalism by Ahlrichs and Brode [20], angular-velocity Verlet method in matrix- and quaternion-constraint schemes [21, 25], and the atomic-constraint technique [11, 17]. All the algorithms took almost the same computer time per step and near 97% of the total time were spent to evaluate pair interactions.

The results obtained for the total energy fluctuations \mathcal{E} as functions of the length of the NVE simulations are shown in Fig. 1 at four fixed step sizes, $h = 1, 2, 3$ and 4 fs. Note that a step size of 2 fs is normally used [31] to simulate water within the atomic-constraint approach. As was expected, the Gear algorithm, being of higher-order in truncations errors, generated more precise trajectories at tiny step sizes ($h < 1$ fs). However, it seems to be unstable already for the least time step presented ($h = 1$ fs, subset (a) of the figure) and leads to the worst results at greater step sizes (see, for example, the case $h = 2$ fs in subset (b)). Somewhat better pattern is observed in the Fincham's leapfrog (marked simply "leapfrog" in Fig. 1) and pseudo-site schemes. But the results are rather poor at moderate and great time steps, $h \geq 2$ fs (subsets (b)–(d)). Much more stable trajectories are produced by the velocity-Verlet integrator within quaternion- and matrix-constraint schemes which exhibit similar equivalence in the energy conservation.

One can see from the figure, only the atomic-constraint and our advanced leapfrog algorithms can be related to long-term stable schemes. The quaternion and principal-axes versions of the last integrator conserved the energy approximately with the same accuracy. For this reason only the result corresponding to quaternion variables is plotted in Fig. 1 to simplify the graph. The leapfrog trajectories have been generated applying quasianalytical solutions (Eqs. (14) and (21)) for angular velocities. The exact solutions obtained by means of iterations of Eq. (7) were calculated also to compare with the quasianalytical values. No deviations between the both results have been identified up to $h = 6$ fs. They differed on each step by uncertainties of order round-off errors only, so that the quasianalytical hypothesis appears to be in an excellent accord.

No shift of the total energy and temperature was observed during advanced leapfrog trajectories at $h \leq 5$ fs over a length of 10 000 time steps. We have obtained the following levels of \mathcal{E} at the end of these trajectories: 0.0016, 0.0065, 0.015, 0.029, 0.049 and 0.10 %, corresponding to $\Upsilon \approx 0.29, 1.2, 2.7, 5.2, 8.7$ and 18 % at $h = 1, 2, 3, 4, 5$ and 6 fs, respectively (for the system under consideration $\mathcal{U} \approx 0.56\%$). Therefore, a step size of 4 fs is still suitable for precise calculations. The greatest time steps 5 fs and 6 fs can sometimes be acceptable in actual simulations, when the precision is not so important, for example, for the equilibration of configurations. The ratio Υ in the interval $h \leq 5$ fs can be fitted with a great accuracy to the function Ch^2 with the coefficient $C \approx 0.29\% \text{ fs}^{-2}$. This is completely in line with the square growth of global errors and, as a consequence, $\mathcal{E}(t)$ at $t \gg h$. All other approaches (except the Gear integrator) exhibited the square growth at sufficiently small h as well. However, only the advanced leapfrog algorithm has provided a minimum of C and, as a consequence, the best total energy conservation.

Such a conservation can even be improved considerable applying a better estimation of on-step velocities. Despite the usual second-order estimators (22) and (25) are in the self-consistency with the same order of global errors, an additional portion is involved into the main term of uncertainties increasing the coefficient C with no relation to the real accuracy of the computed trajectory. Although various more accurate estimators are available [32] to decrease C , they increase significantly coefficients at higher powers of h in the global errors. This makes the simulations unusable for moderate and large step sizes. The influence of higher order terms on the long-time stability in this case cannot be predicted analytically *a priori*, and should rather be measured numerically. We have established that among higher-order estimators only the following four-point symmetric scheme

$$\mathbf{V}(t) = \frac{1}{16} \left[-\mathbf{V}(t - \frac{3h}{2}) + 9\mathbf{V}(t - \frac{h}{2}) + 9\mathbf{V}(t + \frac{h}{2}) - \mathbf{V}(t + \frac{3h}{2}) \right] + \mathcal{O}(h^4) \quad (31)$$

can be recommended for the calculation of on-step velocities $\mathbf{V} \equiv \{\mathbf{v}_i, \boldsymbol{\Omega}_i\}$ within our leapfrog framework. It is understood, of course, that mid-step velocities in the right-hand site of Eq. (31) are already defined quantities. Thus, the computation of the total energy E at time t becomes possible, when the velocity step $t + \frac{3h}{2}$ has been passed and

the potential energy $U(t)$ (known at this stage already at $t + h$) has been taken from memory. The corresponding results for \mathcal{E} , obtained in such a way, are plotted in Fig. 1 by the boldest curves marked as "modified leapfrog". In this case, the total-energy fluctuations decrease about in 1.5 times with respect to the usual two-point scheme. However, the retarded calculation of the total energy requires the previous potential energy and the velocities from three previous steps to be stored in memory.

B. Canonical-ensemble simulations

In the temperature-constant (NVT) dynamics the temperature is conserved exactly by construction and the effect of increasing step sizes on the precision of produced trajectories can be investigated by measuring other relevant functions of the system and comparing them with exact quantities. In our canonical- and microcanonical-ensemble simulations the following thermodynamic quantities were evaluated every step and averaged: total energy, potential energy, temperature, specific heat at constant volume, and mean-square forces and torques. The structure of the TIP4P water was investigated by determining the oxygen-oxygen and hydrogen-hydrogen radial distribution functions (RDFs). Center-of-mass (CM) and angular-velocity (AV) time autocorrelation functions (TAFs) were also found. Orientational relaxation was studied by evaluating the molecular dipole-axis (DA) autocorrelations. To reduce statistical noise, all the measurements were taken over 20 000 time steps. The NVE simulation, performed within the atomic-constraint technique at $h = 2$ fs, was considered as a benchmark against which other algorithms and step sizes are to be compared.

First of all, to finish the discussion with the NVE integrators, we report that deviations in all the measured functions with respect to their benchmark values were in a complete agreement with the corresponding relative deviations Υ in the total energy conservation. For example, the results obtained with the help of the advanced leapfrog algorithm at $h = 2$ fs were indistinguishable from the benchmark ones. At the same time, they differed as large as around 5%, 10% or even 20% with increasing the time step to 4 fs, 5 fs or 6 fs, respectively, however, these differences were smaller than in the case of other integrators. Therefore, there is a little point in pursuing the energy-

conserving algorithms to time steps larger than 5 fs because the deviations become evident.

What about the NVT simulations? They have been performed using explicit and implicit algorithms [24] as well as the advanced leapfrog integrator within the quaternion representation. To our knowledge, no other temperature-constrained algorithms of rotational motion are available. The mean values $\langle U \rangle$ of the potential energy and the specific heat per particle of the system at constant volume $C_V = \partial \langle E \rangle_V / \partial T = k_B [3N + (\langle U^2 \rangle - \langle U \rangle^2) / (k_B T)^2]$, obtained at different time steps, and their relative deviations from the benchmark values $\langle U \rangle = 41.09 \text{ kJ mol}^{-1}$ and $C_V/Nk_B = 10.48$ are collected in Table 1. As can be seen, the results for the explicit algorithm are rather unsatisfactory. For instance, at $h = 4$ fs it has produced an anomalously ordered state of water with a lower energy and very large specific heat. A significantly better pattern is observed in the case of the implicit algorithm in agreement with conclusions of paper [24]. Turning to the advanced algorithm, it is clear that even with the very large time step of 10 fs, the thermodynamic results agree with the benchmark within a percent or two. No drift of the potential energy and other investigated quantities was identified for the advanced algorithm at $h \leq 10$ fs. Somewhat greater deviations in C_V at small step sizes can be explained by the influence of statistical noise due to the finiteness of the observation time. At the fixed number of time steps, such an influence increases with decreasing h .

Correlation functions, calculated during the usual implicit [24] and advanced NVT integrations at different step sizes ($h = 2\text{--}10$ fs) are shown in Fig. 2 in comparison with the benchmark results. In the case of the advanced integrator, the RDFs are practically identical with the benchmark at $h \leq 8$ fs as are CM, AV and DA TAFs. Note that these functions at $h = 4$ and 6 fs coincide completely with those corresponding to $h = 2$ fs and they are not shown in subsets (a)–(c), to simplify the graph. The deviations of the time correlation functions within the usual implicit algorithm are clearly worse. The orientational correlation function (see subset (d)) is to show a systematic discrepancy in this case. For instance, these deviations at $h = 4$ fs are as big as those obtained during the advanced leapfrog integration at $h = 8$ fs. Therefore, the last approach allows a step size approximately twice larger than the usual implicit integrator. This is

very important in actual simulations of large systems, because small step sizes require more expensive computer time to cover the required volume in phase space. A reason of this gain in time is due to applying the mid-step, instead of on-step, scheme for the conservation of temperature. This avoids additional uncertainties caused by using estimators for on-step velocities. As can be seen from the Fig. 2, the advanced leapfrog integrator allows to be used even with a huge time step of 10 fs, given that then there is no detectable difference in RDFs and the CM and AV TAFs are also close.

In the advanced NVT algorithm, the principal angular velocities converged at each step to a relative tolerance of 10^{-6} in average from 5 to 10 iterations with varying the step size from 2 fs to 10 fs. Our calculations were carried out with the tolerance of 10^{-10} that required to perform in average from 8 till 16 iterations for $h = 2\text{--}10$ fs. This contributed a negligible small portion additionally into the total computer time. The convergence of the iterations was observed up to $h = 12$ fs. For the usual implicit leapfrog algorithm, the standard iterative procedure for quaternion components begins to diverge already at $h > 8$ fs. To handle the simulations in this case, special efforts for the convergence has been applied.

In view of the results obtained in this subsection, we can stay that at present time the interval of 10 fs should be considered as an upper step size in reliable NVT simulations on water at room temperatures. Can this practical limit be improved in future, for example, by using a better numerical integrator? Such an improvement looks rather doubtful for the following reason. It is quite evident that an arbitrary numerical scheme will work properly at such values h of the time step when the increments in coordinates and velocities during this step are much smaller than the characteristic lengths: a molecular diameter, $d = 2 \max_a (\Delta_a^2)^{1/2}$, an angle of 1 radian, heat translational, $v = (3k_B T/m)^{1/2}$, and rotational $\Omega = (k_B T(1/J_X + 1/J_Y + 1/J_Z))^{1/2}$ velocities, i.e., when

$$\begin{aligned} \langle [\mathbf{r}_i(t+h) - \mathbf{r}_i(t)]^2 \rangle &\ll d^2, & \langle [\mathbf{v}_i(t+h) - \mathbf{v}_i(t)]^2 \rangle &\ll v^2, \\ \langle \varphi_i^2(t, h) \rangle &\ll 1, & \langle [\boldsymbol{\Omega}_i(t+h) - \boldsymbol{\Omega}_i(t)]^2 \rangle &\ll \Omega^2. \end{aligned} \tag{32}$$

Therefore, to estimate an upper theoretical limit h^* for the step size, it is necessary to increase h and observe when at least one of four inequalities in (32) will

break completely. In water, the translational dynamical variables are much slower with respect to fast orientational degrees of freedom. Further, owing to the low moments of inertia of the molecule and the large torques, only the last condition $\langle [\Omega_i(t+h^*) - \Omega_i(t)]^2 \rangle = \langle [\Omega_i(t+\frac{1}{2}h^*) - \Omega_i(t-\frac{1}{2}h^*)]^2 \rangle \sim \Omega^2$ really will participate in the definition of h^* . Our computations, performed with the help of the advanced leapfrog integrator using the tiny step size of 1 fs to reduce the influence of truncation errors to a minimum, have showed that this condition is fulfilled just as far as $h^* \sim 10$ fs. Even if we imagine a hypothetical situation when the equations of motion are solved exactly at arbitrary h , the simulations with step sizes greater than 10 fs may have not so important meaning in practical applications. This is so, because relevant time correlation functions decay during the 10 fs period in a characteristic way (for example, the AV TAF decreases more than twice). Then, such a time discreteness will lead to the loss of information about these functions at molecular length scales, resulting in a distorting of investigated quantities such as the rotational diffusion coefficient, frequency-dependent dielectric permittivity and others.

V. SUMMARY

We have formulated a new approach for the numerical integration of the equations of motion for systems with interacting rigid bodies. Unlike other standard methods, the principal angular velocities are involved directly into the integration within our approach. The algorithm derived is categorized as a rotational leapfrog, since the variables saved are mid-step angular velocities and on-step orientational positions. The orientations can be expressed in terms of either quaternions or entire rotational matrices. The propagation of velocity- and orientation-dependent quantities to the corresponding middle time points was done using a simple averaging over the two nearest neighboring values that is in the spirit of the leapfrog idea as well. As a result, the following significant benefits have been achieved: (a) the exact conservation of rigid structures appears to be an intrinsic feature of the algorithm, and (b) all the evaluations are performed analytically, without involving any iterative procedures. The relative simplicity of the angular-velocity scheme has made possible also to introduce a thermostatted version

and resolve a problem on the integration of motion for polyatomic molecules with charged sites in the presence of an external inhomogeneous electromagnetic field.

It has been shown on the basis of an actual computer experiment on water that the algorithm presented exhibits noticeably better stability properties than those observed in all other rigid-motion integrators known. Being thermostatted it has allowed to reproduce correct results with time steps which are very close to the upper theoretical limit. The algorithm can easily be implemented for arbitrary rigid bodies and substituted into existing program codes. It seems to be the best choice for long term and great step size MD simulation of large systems with rigid polyatomic molecules.

Acknowledgements. The author would like to acknowledge financial support by the President of Ukraine.

Appendix A. Local and global errors

The order of approximation for algorithms appears to be not so simple question, which was very confused and persistently misinterpreted in the literature. An interesting analysis of this problem was recently done [33] for the translational-motion leapfrog algorithm. In particular, it has been concluded that contrary to the conventional point of view, the order of local errors for this leapfrog is four rather than three for both coordinates and velocities due to a fortunate cancellation of truncation errors during two neighboring time steps. Such a conclusion was based on the fact that any trajectory produced by the standard leapfrog scheme (6) satisfies the relations

$$\begin{aligned}\mathbf{v}_i(t + \frac{3h}{2}) &= 2\mathbf{v}_i(t + \frac{h}{2}) - \mathbf{v}_i(t - \frac{h}{2}) + h [\mathbf{f}_i(t + h) - \mathbf{f}_i(t)]/m, \\ \mathbf{r}_i(t + 2h) &= 2\mathbf{r}_i(t + h) - \mathbf{r}_i(t) + h^2 \mathbf{f}_i(t + h)/m.\end{aligned}\tag{A1}$$

It can be verified easily that the predictors given by Eq. (A1) are accurate to fourth order in time step with respect to truncation errors. The second line of Eq. (A1) exactly represents the well-known Störmer formula, whereas the first one can be considered as its velocity analog within the same fourth-order accuracy (note that $h [\mathbf{f}_i(t + h) - \mathbf{f}_i(t)] = h^2 \dot{\mathbf{f}}_i(t + h/2) + \mathcal{O}(h^4)$).

Using Eqs. (7) and (11), similar relations can be obtained for orientational variables,

$$\begin{aligned}\boldsymbol{\Omega}_i(t + \frac{3h}{2}) &= 2\boldsymbol{\Omega}_i(t + \frac{h}{2}) - \boldsymbol{\Omega}_i(t - \frac{h}{2}) + h \mathbf{J}^{-1} [\mathbf{L}_i(t + h) - \mathbf{L}_i(t)], \\ \mathbf{S}_i(t + 2h) &= 2\mathbf{S}_i(t + h) - \mathbf{S}_i(t) + h^2 \boldsymbol{\Xi}_i(t + h),\end{aligned}\tag{A2}$$

where \mathbf{L}_i is defined according to Eq. (26) and

$$\begin{aligned}\boldsymbol{\Xi}_i(t + h) &= \left\{ [\mathbf{I} - \frac{h}{2} \mathbf{H}_i(t + \frac{3h}{2})]^{-1} [\mathbf{I} + \frac{h}{2} \mathbf{H}_i(t + \frac{3h}{2})] - 2\mathbf{I} \right. \\ &\quad \left. + [\mathbf{I} + \frac{h}{2} \mathbf{H}_i(t + \frac{h}{2})]^{-1} [\mathbf{I} - \frac{h}{2} \mathbf{H}_i(t + \frac{h}{2})] \right\} \mathbf{S}_i(t + h)/h^2.\end{aligned}\tag{A3}$$

These relations are also fourth order and, thus, the same order for local errors is reproduced for \mathbf{S}_i and $\boldsymbol{\Omega}_i$ too within our advanced leapfrog scheme, despite the second order of propagations (8) and (10). The reason for this results again from a cancellation of errors arising in coordinates and velocities during the integration process. Such an increasing of order of the approximation should be considered as an additional positive feature of the algorithm which can explain its long-term stability properties.

Equalities (A2) are, in fact, variants of the same Störmer formula within $\mathcal{O}(h^4)$ accuracy. Indeed, let $\mathbf{U}_i(t) = \mathbf{K}_i(t) + \mathbf{W}(\boldsymbol{\Omega}_i(t)) \mathbf{J} \boldsymbol{\Omega}_i(t)$ be the exact full torque acting on molecule i at time t , where \mathbf{J} denotes the diagonal matrix of principal moments of inertia. Then replacing this function by its approximate counterpart $\mathbf{L}_i(t)$, we involve errors of order $\mathcal{O}(h^2)$, i.e.,

$\mathbf{U}_i(t) - \mathbf{L}_i(t) = \mathcal{O}(h^2)$, whereas $h[\mathbf{L}_i(t+h) - \mathbf{L}_i(t)] = h[\mathbf{U}_i(t+h) - \mathbf{U}_i(t)] + \mathcal{O}(h^4) = h^2 \dot{\mathbf{U}}_i(t + \frac{h}{2}) + \mathcal{O}(h^4)$. Further, expanding the right-hand side of Eq. (A3) into Taylor series with respect to h and neglecting terms of order $\mathcal{O}(h^2)$ and higher yields $\Xi_i(t+h) = [(\mathbf{H}_i(t + \frac{3h}{2}) - (\mathbf{H}_i(t + \frac{h}{2}))/h + (\mathbf{H}_i^2(t + \frac{3h}{2}) + (\mathbf{H}_i^2(t + \frac{h}{2}))/2] \mathbf{S}_i(t+h) + \mathcal{O}(h^2) = \ddot{\mathbf{S}}_i(t+h) + \mathcal{O}(h^2)$, where $\ddot{\mathbf{S}}_i(t+h) = \frac{d}{dt} \dot{\mathbf{S}}_i(t+h) = \frac{d}{dt} (\mathbf{H}_i(t+h) \mathbf{S}_i(t+h)) = [\mathbf{H}(\dot{\mathbf{\Omega}}_i(t+h)) + \mathbf{H}_i^2(t+h)] \mathbf{S}_i(t+h)$ with $\dot{\mathbf{\Omega}}_i(t+h) = \mathbf{J}^{-1} \mathbf{U}_i(t+h)$.

The local errors are only a part of the story, because they accumulate step by step thus producing so-called global errors. For the translational leapfrog algorithm it has been shown [33] that the characteristic square growth in global deviations of the total energy with increasing the step size can be a result of additional interpolation errors appearing in second-order estimator (22) of on-step kinetic energy with no relation to the accuracy of the computed trajectory. If higher order estimators (like (31)) are used, the global error in the total energy must be between $\mathcal{O}(h^2)$ and $\mathcal{O}(h^3)$ but it depends upon specific properties of the equations of motion. This conclusion is valid for the advanced angular-velocity algorithm as well. The last statement can briefly be grounded as follows.

First of all, it is worth remarking that equations (6) and (A1) as well as Eqs. (7), (8), (11) and (A2) are not equivalent. Eqs. (A1) and (A2) provide a leapfrog solution only if initial values for the pairs $\mathcal{P}_1 \equiv \{\mathbf{r}_i(t), \mathbf{S}_i(t), \mathbf{v}_i(t - \frac{h}{2}), \mathbf{\Omega}_i(t - \frac{h}{2})\}$ and $\mathcal{P}_2 \equiv \{\mathbf{r}_i(t+h), \mathbf{S}_i(t+h), \mathbf{v}_i(t + \frac{h}{2}), \mathbf{\Omega}_i(t + \frac{h}{2})\}$ match Eqs. (6), (7), (8) and (11). Starting from arbitrary initial conditions, a completely non-leapfrog trajectory can be produced by (A1) and (A2) (for example, the matrices $\mathbf{S}_i(t+2h)$ can be not orthonormal in this case). For the same reason, we should treat the increasing order of truncation errors to four in somewhat conditional meaning. Indeed, let the point \mathcal{P}_1 belongs the exact trajectory. Then at the start of the integration process (A1) and (A2) the point \mathcal{P}_2 , according to the single leapfrog step, will be localized in phase space within errors of order $\mathcal{O}(h^3)$ and these errors in its turn will be transferred step by step in the produced trajectory. Therefore, we can talk about $\mathcal{O}(h^4)$ local deviations with respect to the exact trajectory which was perturbed initially by $\mathcal{O}(h^3)$ uncertainties. To reach the pure third order in global errors of energy, such a perturbation must be avoided. This requires that the exact trajectory passes (at least within $\mathcal{O}(h^4)$ accuracy) through the both leapfrog states \mathcal{P}_1 and \mathcal{P}_2 . However, since we have only two translational and two rotational first-order equations of motion per molecule, this exact solution does not necessarily exist. In the general case, even specially choosing initial point \mathcal{P}_1 , one can fit precisely either the leapfrog coordinates $\{\mathbf{r}_i(t+h), \mathbf{S}_i(t+h)\}$ or velocities $\{\mathbf{v}_i(t + \frac{h}{2}), \mathbf{\Omega}_i(t + \frac{h}{2})\}$ to the corresponding exact values.

Appendix B. The integration in the presence of external fields

Consider, finally, how to perform the integration in the presence of external electromagnetic fields. The electric field $\mathbf{E}(\mathbf{r}, t)$ involves additional terms, $\mathbf{f}_i^E(t) = \sum_a^M e_a \mathbf{E}(\mathbf{r}_i^a, t)$ and $\mathbf{K}_i^E(t) = \mathbf{A}_i(t) \sum_a^M e_a \mathbf{E}(\mathbf{r}_i^a, t) \times (\mathbf{r}_i^a - \mathbf{r}_i)$ with e_a being the charge of site a , which must be included correspondingly into the usual molecular forces $\mathbf{f}_i(t)$ and principal torques $\mathbf{K}_i(t)$ caused by interparticle interactions. These terms can easily be evaluated at time t using translational $\mathbf{r}_i(t)$ and orientational $\mathbf{S}_i(t)$ coordinates. Analogous terms involved by the magnetic field $\mathbf{B}(\mathbf{r}, t)$ and needed for the inclusion as well are: $\mathbf{f}_B(\mathbf{v}_i(t), \boldsymbol{\Omega}_i(t), t) = \frac{1}{c} \sum_a^M e_a \mathbf{v}_i^a(t) \times \mathbf{B}(\mathbf{r}_i^a, t)$ and $\mathbf{K}_B(\mathbf{v}_i(t), \boldsymbol{\Omega}_i(t), t) = \mathbf{A}_i(t) \frac{1}{c} \sum_a^M e_a [\mathbf{v}_i^a(t) \times \mathbf{B}(\mathbf{r}_i^a, t)] \times (\mathbf{r}_i^a - \mathbf{r}_i)$, where c is the light velocity. They depend on both translational and angular velocities, because velocities of individual atoms \mathbf{v}_i^a are evaluated using the velocity due to rotation alone, determined in the body frame, then transformed into the lab frame and added to the velocity of the center of mass: $\mathbf{v}_i^a(t) = \mathbf{v}_i(t) + \mathbf{A}_i^+(t) [\boldsymbol{\Omega}_i(t) \times \boldsymbol{\Delta}^a]$.

Collecting the free-motion contributions $(J_\beta - J_\gamma) \Omega_\beta^i \Omega_\gamma^i \equiv [\mathbf{W}(\boldsymbol{\Omega}_i) \mathbf{J} \boldsymbol{\Omega}_i]_\alpha$ of the torques together with the magnetic-field terms into the vector $\mathbf{M}(\mathbf{v}_i(t), \boldsymbol{\Omega}_i(t), t) = \mathbf{K}_B(\mathbf{v}_i(t), \boldsymbol{\Omega}_i(t), t) + \mathbf{W}(\boldsymbol{\Omega}_i(t)) \mathbf{J} \boldsymbol{\Omega}_i(t)$, the velocity part of the algorithm can be proceeded as follows

$$\begin{aligned} \mathbf{v}_i^{(n+1)}(t + \frac{h}{2}) &= \mathbf{v}_i(t - \frac{h}{2}) + \frac{h}{m} [\mathbf{f}_i(t) + \mathbf{f}_i^E(t) + \mathbf{f}_B^{(n)}(t)], \\ \boldsymbol{\Omega}_i^{(n+1)}(t + \frac{h}{2}) &= \boldsymbol{\Omega}_i(t - \frac{h}{2}) + h \mathbf{J}^{-1} [\mathbf{K}_i(t) + \mathbf{K}_i^E(t) + \mathbf{M}^{(n)}(t)], \end{aligned} \quad (\text{B1})$$

where

$$\begin{aligned} \mathbf{f}_B^{(n)}(t) &= \frac{1}{2} [\mathbf{f}_B(\mathbf{v}_i(t - \frac{h}{2}), \boldsymbol{\Omega}_i(t - \frac{h}{2}), t) + \mathbf{f}_B(\mathbf{v}_i^{(n)}(t + \frac{h}{2}), \boldsymbol{\Omega}_i^{(n)}(t + \frac{h}{2}), t)], \\ \mathbf{M}^{(n)}(t) &= \frac{1}{2} [\mathbf{M}(\mathbf{v}_i(t - \frac{h}{2}), \boldsymbol{\Omega}_i(t - \frac{h}{2}), t) + \mathbf{M}(\mathbf{v}_i^{(n)}(t + \frac{h}{2}), \boldsymbol{\Omega}_i^{(n)}(t + \frac{h}{2}), t)] \end{aligned} \quad (\text{B2})$$

are the propagation for velocity-dependent parts of the forces and torques to on-step levels of time. Equalities (B1) lead to a system of six coupled equations per molecule for six unknowns, namely, for three components of translational $\mathbf{v}_i(t + \frac{h}{2})$ and angular $\boldsymbol{\Omega}_i(t + \frac{h}{2})$ velocities. The system can now be solved using iterations ($n = 0, 1, \dots$) separately for each molecule and putting initially $\mathbf{v}_i^{(0)}(t + \frac{h}{2}) = \mathbf{v}_i(t - \frac{h}{2})$ and $\boldsymbol{\Omega}_i^{(0)}(t + \frac{h}{2}) = \boldsymbol{\Omega}_i(t - \frac{h}{2})$. The evaluation of coordinates $\mathbf{r}_i(t + h)$ and $\mathbf{S}_i(t + h)$ is performed in view of the second line of Eq. (6) and Eq. (12), i.e., quite analogously to the case when electromagnetic fields are absent.

REFERENCES

- [1] H. Goldstein, Classical Mechanics (Addison-Wesley, Reading, Massachusetts, 1980).
- [2] J. Barojas, D. Levesque, and B. Quentrec, Simulation of diatomic homonuclear liquids, *Phys. Rev.* 1092, **A 7** (1973).
- [3] D. Levesque, J.J. Weis, and G.N. Patey, Fluids of Lennard-Jones spheres with dipoles and tetrahedral quadrupoles. A comparison between computer simulation and theoretical results, *Mol. Phys.* 333, **51** (1984).
- [4] D.J. Evans, On the representation of orientation space, *Mol. Phys.* 317, **34** (1977).
- [5] M.P. Allen and D.J. Tildesley, Computer Simulation of Liquids (Oxford Science Press, Oxford, 1987).
- [6] D.C. Rapaport, The Art of Molecular Dynamics Simulation (Cambridge University Press, Cambridge, 1995).
- [7] C.W. Gear, Numerical Initial Value Problems in Ordinary Differential Equations (Prentice-Hall, Engelwood Cliffs, NJ, 1971).
- [8] A. Rahman and F.H. Stillinger, Molecular dynamics study of liquid water, *J. Chem. Phys.* 3336, **55** (1971).
- [9] D.J. Evans and S. Murad, Singularity free algorithm for molecular dynamics simulation of rigid polyatomics, *Mol. Phys.* 327, **34** (1977).
- [10] J.P. Ryckaert and A. Bellemans, Molecular dynamics of liquid *n*-butane near its boiling point, *Chem. Phys. Lett.* 123, **30** (1975).
- [11] G. Ciccotti, M. Ferrario, and J.P. Ryckaert, Molecular dynamics of rigid systems in cartesian coordinates. A general formulation, *Mol. Phys.* 1253, **47** (1982).
- [12] L. Verlet, Computer experiments on classical fluids. I. Thermodynamic properties of Lennard-Jones molecules, *Phys. Rev.* 98, **159** (1967).
- [13] W.C. Swope, H.C. Andersen, P.H. Berens, and K.R. Wilson, A computer sim-

ulation method for the calculation of equilibrium constants for the formation of physical clusters of molecules: Application to small water clusters, *J. Chem. Phys.* 637, **76** (1982).

[14] R.W. Hockney and J.W. Eastwood, Computer Simulation Using Particles (McGraw-Hill, New York, 1981).

[15] D. Beeman, Some multistep methods for use in molecular dynamics calculations, *J. Comput. Phys.* 130, **20** (1976).

[16] G.D. Venneri and W.G. Hoover, Simple exact test for well-known molecular dynamics algorithms, *J. Comput. Phys.* 486, **73** (1987).

[17] J.P. Ryckaert, G. Ciccotti, and H.J.C. Berendsen, Numerical integration of the Cartesian equations of motion of a system with constraints: Molecular dynamics of *n*-alkanes, *J. Comput. Phys.* 327, **23** (1977).

[18] H.C. Andersen, Rattle: a ‘velocity’ version of the shake algorithm for molecular dynamics calculations, *J. Comput. Phys.* 24, **52** (1983).

[19] B.J. Leimkuhler and R.D. Skeel, Symplectic numerical integrators in constrained Hamiltonian systems, *J. Comput. Phys.* 117, **112** (1994).

[20] R. Ahlrichs, and S. Brode, A new rigid motion algorithm for MD simulations, *Comput. Phys. Commun.* 59, **42** (1986).

[21] I.P. Omelyan, Numerical integration of the equations of motion for rigid polyatomics: The matrix method, *Comput. Phys. Commun.* 171, **109** (1998).

[22] A. Kol, B. Laird, and B. Leimkuhler, A symplectic method for rigid-body molecular simulation, in Numerical Analysis Reports (University of Cambridge, DAMTP 1997/NA5), 19 p.

[23] D. Fincham, An algorithm for the rotational motion of rigid molecules, *CCP5 Information Quarterly* 6, **2** (1981).

[24] D. Fincham, Leapfrog rotational algorithms, *Mol. Simul.* 165, **8** (1992).

- [25] I.P. Omelyan, On the numerical integration of motion for rigid polyatomics: The modified quaternion approach, *Computers in Physics* 97, **12** (1998).
- [26] I.P. Omelyan, Algorithm for numerical integration of the rigid-body equations of motion, *Phys. Rev. E* 1169, **58** (1998).
- [27] D. Fincham, Choice of time step in molecular dynamics simulations, *Comput. Phys. Commun.* 263, **40** (1986).
- [28] D. Brown and J.H.R. Clarke, A comparison of constant energy, constant temperature and constant pressure ensembles in molecular dynamics simulations of atomic liquids, *Mol. Phys.* 1243, **51** (1984).
- [29] W.L. Jorgensen, J. Chandrasekhar, J.D. Madura, R.W. Impey, and M.L. Klein, Comparison of simple potential functions for simulating liquid water, *J. Chem. Phys.* 926, **79** (1983).
- [30] I.P. Omelyan, On the reaction field for interaction site models of polar systems, *Phys. Lett. A* 295, **223** (1996).
- [31] D. Bertolini and A. Tani, Generalized hydrodynamics and the acoustic modes of water: Theory and simulation results, *Phys. Rev. E* 1091, **51** (1995).
- [32] M. Amini and D. Fincham, Evaluation of temperature in molecular dynamics simulation, *Comput. Phys. Commun.* 313, **56** (1990).
- [33] A.K. Mazur, Common molecular dynamics algorithms revisited: Accuracy and optimal time steps of Störmer-leapfrog integrators, *J. Comput. Phys.* 354, **136** (1997).

Table 1. Thermodynamic results for the TIP4P water using explicit, implicit and advanced rotational algorithms incorporating the temperature constraint $T = 298$ K

h/fs	Explicit		Implicit		Advanced	
	Value	Dev. (%)	Value	Dev. (%)	Value	Dev. (%)
POTENTIAL ENERGY / kJ mol^{-1}						
2	-41.28	0.5	-40.99	0.2	-41.26	0.4
4	-46.87	14	-40.73	0.9	-41.21	0.3
6	-41.83	1.8	-40.22	2.1	-41.23	0.3
8	-39.45	4.0	-39.51	3.8	-41.44	0.9
10	-37.74	8.2	-38.36	6.6	-41.98	2.2
12	-34.20	17	-35.07	15	-43.77	6.5
SPECIFIC HEAT at constant volume / Nk_{B}						
2	16.41	57	8.87	15	9.76	6.9
4	438.35	4083	9.89	5.6	9.93	5.2
6	52.94	405	9.89	5.6	10.28	1.9
8	10.87	3.7	10.11	3.5	10.35	1.2
10	12.15	16	11.46	9.4	10.47	0.1
12	53.66	412	16.59	58	12.75	22

Figure captions

Fig. 1. The total energy fluctuations as functions of the length of the NVE simulations on the TIP4P water, performed in various techniques at four fixed time steps: **(a)** 1 fs, **(b)** 2 fs, **(c)** 3 fs and **(d)** 4 fs.

Fig. 2. Oxygen-oxygen (O-O) and hydrogen-hydrogen (H-H) radial distribution functions **(a)**, center-of-mass **(b)** and and angular-velocity **(c)** time autocorrelation functions, and orientational relaxation **(d)**, obtained in NVT simulations of the TIP4P water. The results corresponding to the step sizes $h = 2, 8$ and 10 fs are plotted by bold solid, short-dashed and thin solid curves, respectively. Additional long-short dashed and dashed curves in **(d)** correspond to the cases of $h = 4$ and 6 fs. The sets of curves related to the usual implicit and advanced leapfrog algorithms are labeled as "U" and "A", respectively. The result of the usual implicit algorithm is presented in **(c)** by long-dashed curve for $h = 10$ fs only to simplify the graph. The benchmark data are shown as open circles. Note that the advanced-algorithm curves are indistinguishable in **(d)** at $h = 2, 4$ and 6 fs.

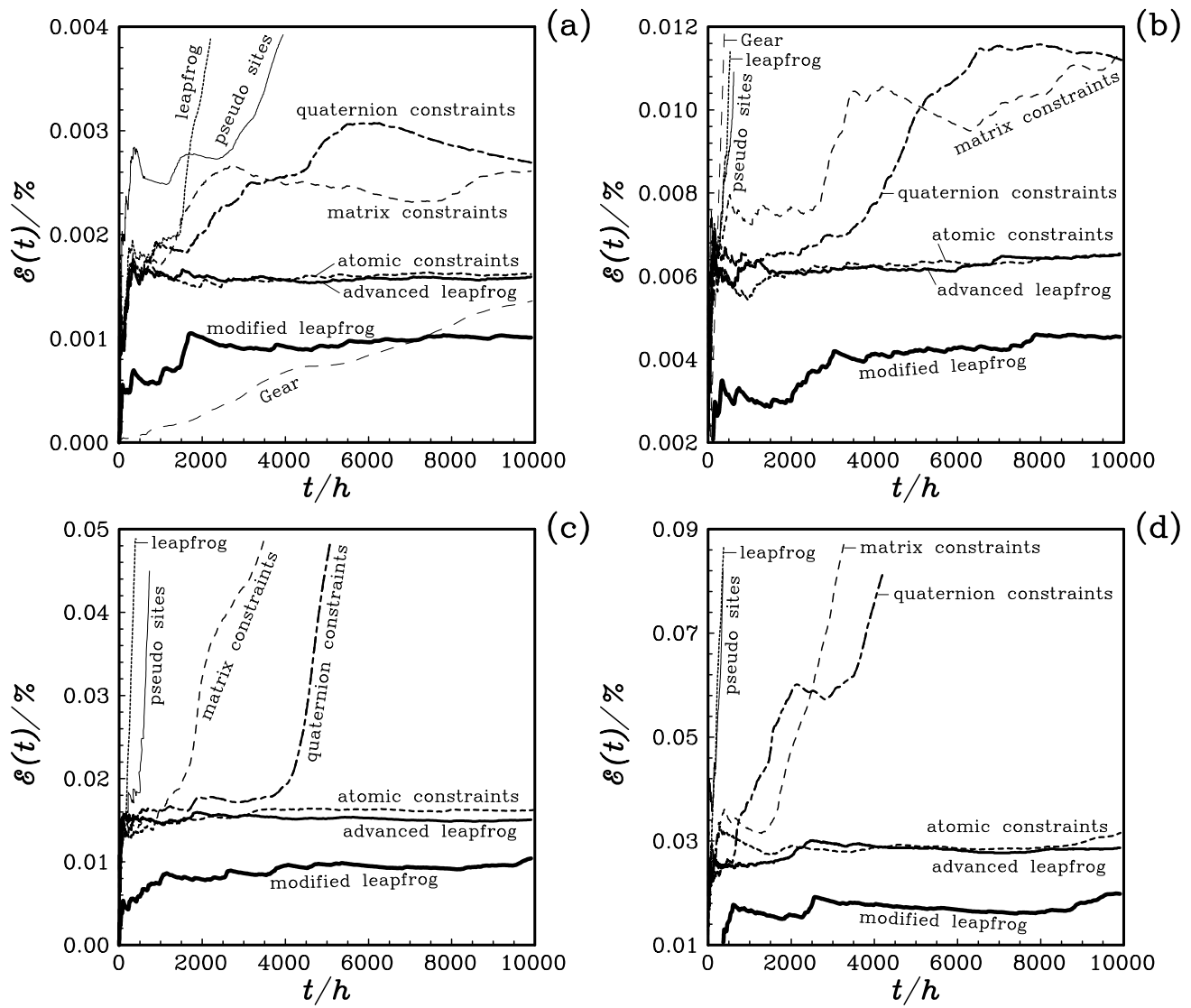


Fig. 1. I.P.Omelyan
Journal of Computational Physics

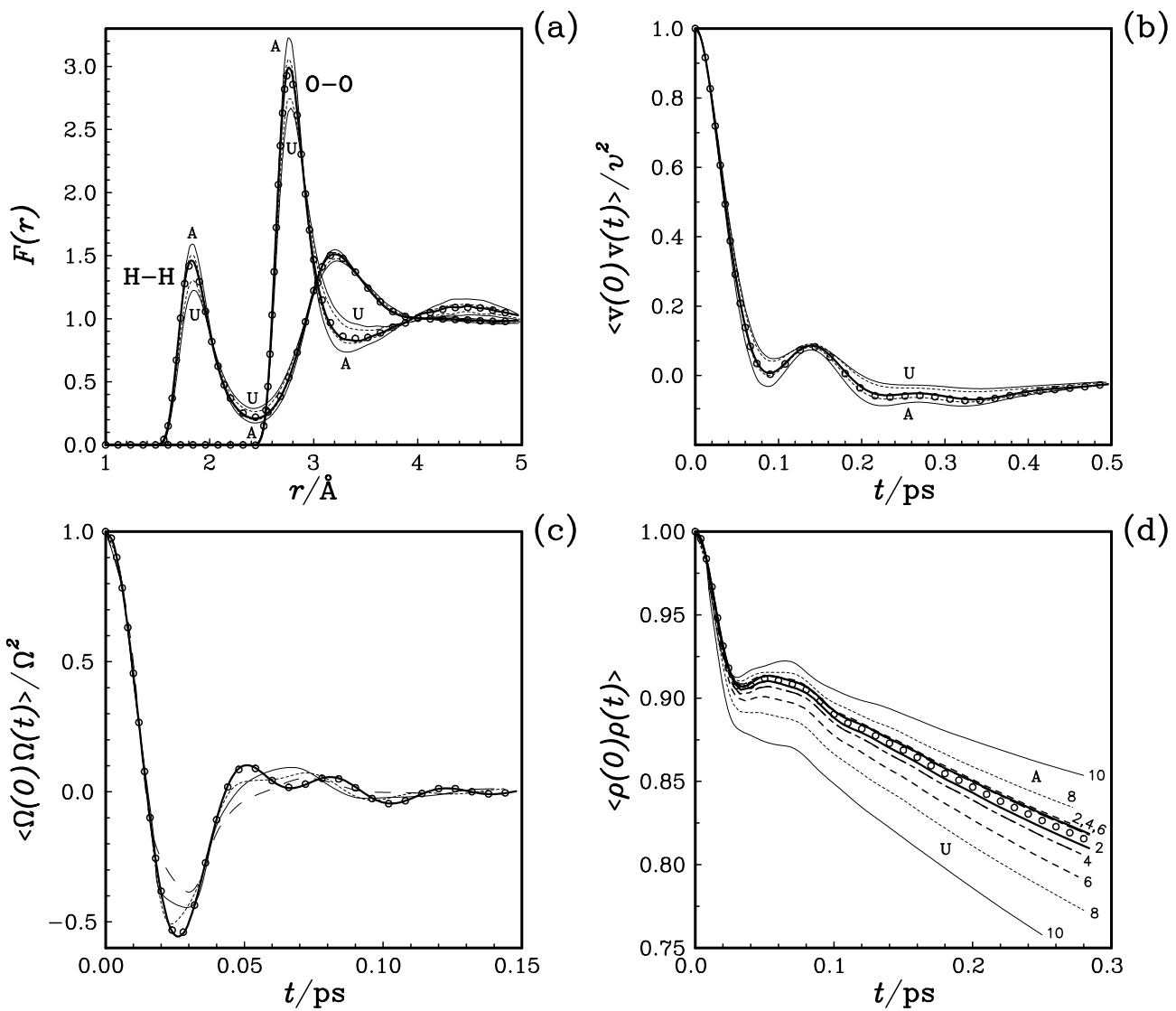


Fig. 2. I.P. Omelyan
Journal of Computational Physics